Journal of Medicinal Chemistry

ARTICLE

pubs.acs.org/jmc

Metal-Based Inhibition of Poly(ADP-ribose) Polymerase — The Guardian Angel of DNA

Filipa Mendes,[†] Michael Groessl,[‡] Alexey A. Nazarov,[‡] Yury O. Tsybin,[‡] Gianni Sava,[§] Isabel Santos,[†] Paul J. Dyson,[‡] and Angela Casini*[,‡]

[†]Unidade de Ciências Químicas e Radiofarmacêuticas, Instituto Tecnológico e Nuclear, Estrada Nacional 10, 2686-953 Sacavém, Portugal

[‡]Institut des Sciences et Ingénierie Chimiques, Ecole Polytechnique Fédérale de Lausanne (EPFL), CH-1015 Lausanne, Switzerland

[§]Callerio Foundation Onlus, Via A. Fleming 22-31, 34127 Trieste, Italy

ABSTRACT:

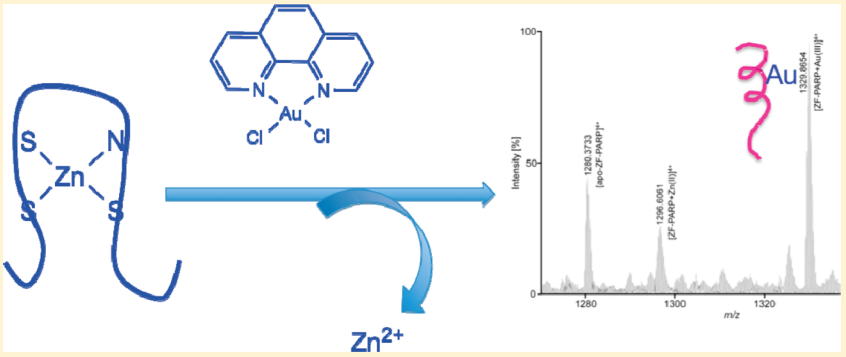

The inhibition activity of a series of anticancer metal complexes based on platinum, ruthenium, and gold metal ions was evaluated on the zinc-finger protein PARP-1, either purified or directly on protein extracts from human breast cancer MCF7 cells. Information on the reactivity of the metal complexes with the PARP-1 zinc-finger domain was obtained by high-resolution ESI FT-ICR mass spectrometry. An excellent correlation between PARP-1 inhibition in protein extracts and the ability of the complexes to bind to the zinc-finger motif (in competition with zinc) was established. The results support a model whereby displacement of zinc from the PARP-1 zinc finger by other metal ions leads to decreased PARP-1 activity. *In vitro* combination studies of cisplatin with NAMI-A and RAPTA-T on different cancer cell lines (MCF7, A2780, and A2780cisR) showed that, in some cases, a synergistic effect is in operation.

INTRODUCTION

Following the discovery of the anticancer properties of cisplatin in 1965 by Rosenberg and co-workers,[1] considerable efforts have been made both to unravel the mechanisms by which it exerts its anticancer effect[2] and to develop alternative metal-based drugs to broaden the range of treatable tumors.[3−5] During the last few decades, the majority of research on anticancer metal-based compounds has focused on their interactions with DNA, since it was recognized to be a primary target for platinum compounds.[2,6,7] However, it is increasingly evident that the interactions of anticancer metallodrugs with enzymes and proteins deserves more attention, since they play important roles in metal complex uptake and biodistribution processes and in determining their overall toxicity profile.[8] The reactions of metal complexes with proteins are also likely to be involved in crucial aspects of their mechanism of action,[9−11] particularly for non-platinum anticancer compounds (*e.g.*, compounds based on ruthenium and gold centers), for which multiple biological pathways have been proposed, including the inhibition of cysteine proteases[12,13] by ruthenium compounds and the inhibition of mitochondrial enzymes by gold complexes.[14,15]

Within this frame, the poly(adenosine diphosphate (ADP)-ribose) polymerases (PARPs) are essential proteins involved in cancer resistance to chemotherapies. PARPs play a key role in DNA repair by detecting DNA strand breaks and catalyzing poly(ADP-ribosylation),[16] and consequently, PARPs have been referred to as "the guardian angels" of DNA.[17] Notably, PARP-1, the most studied member of the PARP family, is characterized by the presence of two long zinc fingers (ZF-PARPs, also termed as nick-sensors) that are positioned upstream of the catalytic domain[18] and mediate specific nicked DNA recognition.[19] Figure 1 shows the structure of the catalytically essential N-terminal ZF-PARP-1 peptide.[20] The enzyme reaction then uses NAD^+ as a substrate and catalyzes the addition of long branching chains of poly(ADP-ribose) polymers to target

Received: October 25, 2010
Published: March 03, 2011

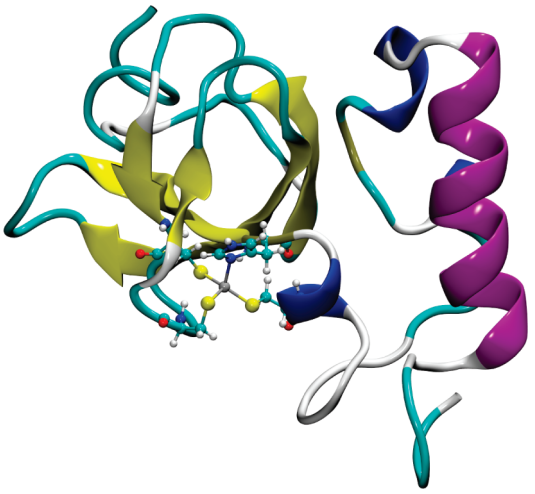

Figure 1. Ribbon representation of the NH_2-terminal zinc finger of PARP-1 (from pdb 2DMJ), with the Zn^{2+} binding motif shown as a ball-and-stick model. The 106 amino acid sequence is as follows: GSSGSSGMAESSDKLYRVEYAKSGRAS**C**KK**C**SESIPKDSLRMAIM VQSPMFDGKVPHWY**H**FS**C**FWKVGHSIRHPDVEVDGFSELRWD DQQKVKKTAEAGGSGPSSG (Zn-binding residues Cys-28, Cys-31, His-60, and Cys-63 in bold letters).

proteins or PARP itself.[21,22] PARP is activated by mild to moderate genotoxic stimuli, which facilitates DNA repair by signaling cell cycle arrest and by interacting with DNA repair enzymes.[21] Severe DNA damage may even induce hyperactivation of PARP, which ultimately leads to apoptosis.[23,24]

PARP inhibitors have been considered as drugs for use in combinatorial therapies with alkylating agents,[25] to sensitize cancer cells to subsequent treatment with cisplatin and carboplatin.[26−29] Indeed, phase I and II clinical trials to evaluate the potential of PARP inhibitors in combination therapies with platinum drugs are currently in progress.[30]

Notably, PARP has been shown to bind to platinum-modified DNA.[31,32] A systematic *in vitro* study was recently conducted in which the effect of PARP inhibition on the ability of nuclear proteins to bind platinum-modified DNA was evaluated by photo-cross-linking experiments.[33] According to these studies, the activity of PARP, following exposure to platinated DNA, resulted in the dissociation of DNA-bound proteins. Moreover, PARP inhibitors were able to sensitize some, but not all, of the cell lines to cisplatin. Other studies describe the binding of PARP-1 to platinum 1,2-d(GpG) and 1,3-d(GpTpG) intrastrand cross-links on duplex DNA,[33,34] and a very recent report demonstrated that PARP-1 differentiates between normal and platinum-damaged DNA, having higher binding affinity for the cisplatin 1,2-d(GpG) cross-links than for the unplatinated DNA or other types of cisplatin-DNA cross-links.[35] In this latter study, it was also shown that PARP-1 may shield the DNA lesion from repair and trigger a cytotoxic response.

Despite these studies, the activity of PARP upon cisplatin treatment remains controversial and not fully understood. Herein, we propose an alternative mechanistic hypothesis in which PARP is a pharmacological target of metal-based drugs. Such a hypothesis is based on the inhibition activity studies of a series of metal-based drugs (platinum, ruthenium, and gold) on purified PARP-1 and on protein extracts from human breast cancer MCF7 cells. Considering that the PARP structure contains ZF motifs that may be altered by the metal complexes, we have also studied the nature

Chart 1. Structures of the Compounds Used in This Study

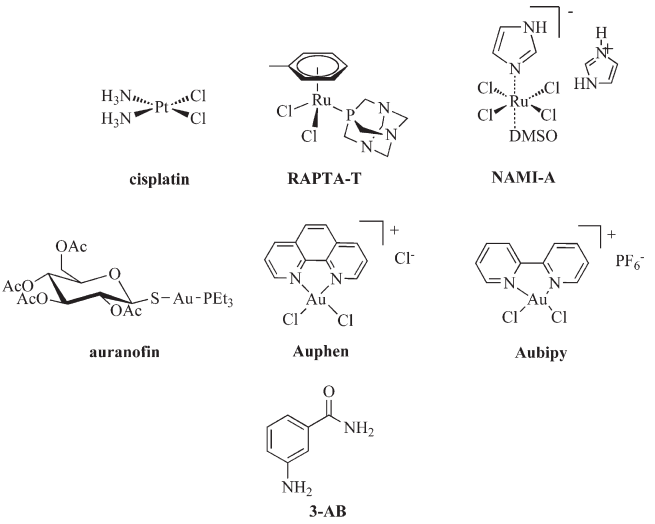

of the possible metal-ZF-PARP adducts by high-resolution electrospray ionization Fourier-transform ion cyclotron mass spectrometry (ESI-FT-ICR MS). An excellent correlation between PARP-1 inhibition and the ability of the complexes to bind to the ZF motif was observed. Moreover, *in vitro* combination studies to evaluate the cooperative effect of PARP-1 inhibition and DNA binding on cytotoxicity are described.

RESULTS AND DISCUSSION

A series of complexes based on ruthenium and gold were investigated for their inhibitory properties of PARP-1 in comparison to cisplatin and 3-aminobenzamide (3-AB),[36] the latter being the benchmark PARP inhibitor (Chart 1). The series included compounds that inhibit invasion processes *in vitro* and show an antimetastatic effect *in vivo*, $[Ru(\eta^6\text{-}p\text{-toluene})Cl_2(pta)]$ (pta = 1,3,5-triaza-7-phosphaadamantane, RAPTA-T)[37−39] and *trans*-[Ru(dmso)(Him)Cl_4]Him (dmso = methylsulfoxide, Him = imidazole, NAMI-A),[40,41] as well as the antirheumatic agent (Au(2,3,4,6-tetra-*O*-acetyl-1-(thio-κS)-β-D-glucopyranosato)PEt_3) (PEt_3 = triethylphosphine, auranofin)[42,43] and the cytotoxic gold(III) compounds $[Au(phen)Cl_2]Cl$[44,45] (phen = 1,10-phenanthroline, Auphen) and $[Au(bipy)Cl_2](PF_6)$[46] (bipy = 2,2′-bipyridine, Aubipy).

PARP-1 inhibition was initially determined on the purified human enzyme. The enzyme was incubated with each compound at various concentrations for 24 h before assessing its activity spectrophotometrically by measuring the incorporation of biotinylated poly(ADP-ribose) onto histone proteins (see the Experimental Section for further details). The long incubation time was selected in order for the compounds to establish maximum inhibition, in particular for the ruthenium complexes that have been previously reported to behave as typical time-dependent enzyme inhibitors.[12] The resulting IC_{50} values are reported in Table 1 in comparison to the PARP-1 reference inhibitor 3-AB. Notably, all the complexes are superior PARP-1 inhibitors compared to 3-AB, with the gold complexes showing the most potent effect and the lowest IC_{50} values (in the nanomolar range), followed by cisplatin ($IC_{50} \sim 12.3\ \mu M$) and the ruthenium complexes.

Incubation of protein cell extracts (isolated from MCF7 cells) with the compounds (50 or 150 μM) for 24 h at 37 °C followed by determination of PARP-1 activity shows that the complexes

dx.doi.org/10.1021/jm2000135 |J. Med. Chem. 2011, 54, 2196–2206

maintain their inhibition activity. Figure 2 shows the residual activity of PARP-1 on protein extracts treated with the complexes and 3-AB at a fixed concentration of 50 μM. The most effective ruthenium compound is NAMI-A, which reduced PARP-1 activity to ca. 21%, with respect to untreated protein extracts. Notably, NAMI-A is more efficient than 3-AB (residual activity = 55%). Cisplatin also inhibits PARP-1 activity (residual activity = 52%), albeit to a lesser extent than NAMI-A, but comparable to that of 3-AB. The least active compound is RAPTA-T (residual activity = 70%). The lower activity of RAPTA-T compared to NAMI-A, relative to their similar inhibition on the purified protein, indicates that RAPTA-T binds preferentially to other protein targets including proteases.[12] Aubipy and Auphen are the most potent compounds of the series, inhibiting PARP-1 activity to ca. 12% of residual activity, with auranofin displaying preferential interactions with other targets, such as the seleno-enzyme thioredoxin reductase.[14]

As mentioned above, overexpression of PARP in cancer cells has been linked to drug resistance and the overall ability of cancer cells to survive genotoxic stress. PARP-1 inhibition has been shown to sensitize tumor cells to chemotherapeutic agents including platinum compounds.[29,47] Therefore, we decided to evaluate the cytotoxic effect of cisplatin administered in combination with different concentrations of RAPTA-T or NAMI-A. The ruthenium complexes were selected for the coadministration experiments, as good PARP-1 inhibition is observed at concentrations significantly below cytotoxic doses, which is relevant to the further development of these compounds in combination therapy *in vivo*. Cisplatin inhibited MCF7 cell proliferation with an $IC_{50} = 20 \pm 3$ μM after 72 h treatment whereas RAPTA-T and NAMI-A were practically nontoxic even at a concentration of 500 μM, as shown in Figure 3.

Figure 3 compares the survival of MCF7 cells treated for 72 h with 25 μM cisplatin or with 25 μM cisplatin together with RAPTA-T or NAMI-A at concentrations of 150, 300, or 500 μM (data obtained on RAPTA-T and NAMI-A treated cells are also reported for comparison). Concerning the relatively high concentrations of the ruthenium complexes used in our study and their relevance to the real *in vivo* situation, it is worth mentioning that, for example, the low cytotoxicity and rather acceptable toxicity profile of NAMI-A allowed administration of relatively high doses of compound to patients enrolled in clinical trials.[48] Moreover, high intracellular concentrations of ruthenium are usually attained both *in vitro* and *in vivo* following NAMI-A treatment, as reported by Sava and co-workers based on atomic absorption determinations.[49] In the reported cell studies, extracellular concentrations of NAMI-A up to 100 μM or even 1 mM were applied and excellent uptake of ruthenium was revealed. Finally, a recent study on the reaction of NAMI-A with serum albumin revealed that NAMI-A/albumin adducts retain a significant biological activity.[50] Thus, ruthenium bound to serum albumin in the cell culture medium might still serve as a drug reservoir at the cancer cell surface.

The results of our experiment show that cisplatin cytotoxicity increases approximately 2-fold when coadministered with (noncytotoxic) 150 μM doses of RAPTA-T and NAMI-A. The cytotoxicity of the combined treatment increases up to 3-fold, with 500 μM doses of the ruthenium drugs.

Statistical analysis based on the method of Chou and Talaly[51] was performed, and in Table 2 a comparison of the predicted *survival rates* (defined as the expected cell viability if the combined activities of the compounds are additive) and the experimentally determined values (the observed viabilities) is reported. The observed survival rates for the combinations of the two ruthenium compounds at different concentrations with cisplatin are significantly lower than those predicted, indicating a synergistic effect between the two compounds is in operation.

Similar coadministration experiments were repeated for the A2780 human ovarian cancer cell lines and the cisplatin resistant analogue, A2780cisR, for which cisplatin has IC_{50} values of 1.9 ± 0.6 μM and 20 ± 5 μM, respectively. It should be noted that RAPTA-T and NAMI-A alone showed a cytotoxic effect on both cell lines at 150 μM. Cells were incubated with 1 or 10 μM cisplatin (for A2780 and A2780cisR, respectively) and different concentrations of RAPTA-T or NAMI-A (150, 300, or 500 μM).

Table 1. IC_{50} Values for PARP-1 Inhibition Following 24 h Incubation

compound	IC_{50} (μM)[a]
RAPTA-T	28 ± 2
NAMI-A	18.9 ± 1.6
cisplatin	12.3 ± 2.0
auranofin	0.079 ± 0.009
Auphen	0.0069 ± 0.0001
Aubipy	0.0077 ± 0.0001
3-AB	33[36]

[a] Values are the mean ± SD of at least three determinations each, performed in triplicate.

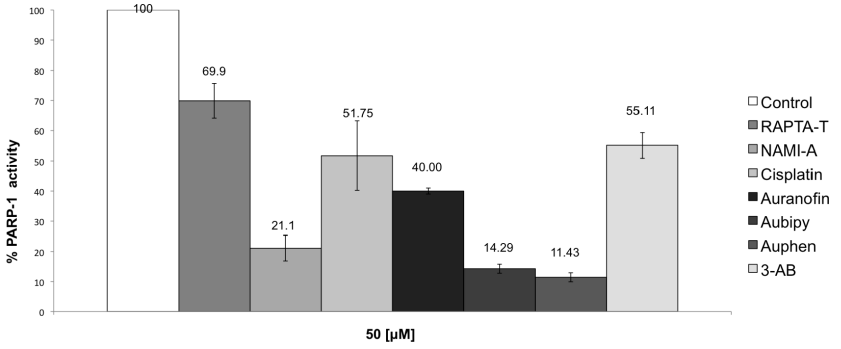

Figure 2. PARP-1 activity levels in MCF7 protein extracts. PARP-1 activity was measured in homogenates (50 μg of protein) treated with the compounds (50 μM) over 24 h at 37 °C, in comparison to the standard inhibitor 3-AB. Data are the mean ± SD of at least three experiments, each performed in triplicate. Tukey−Kramer multiple comparison test: compound $p < 0.01$ vs control in all cases.

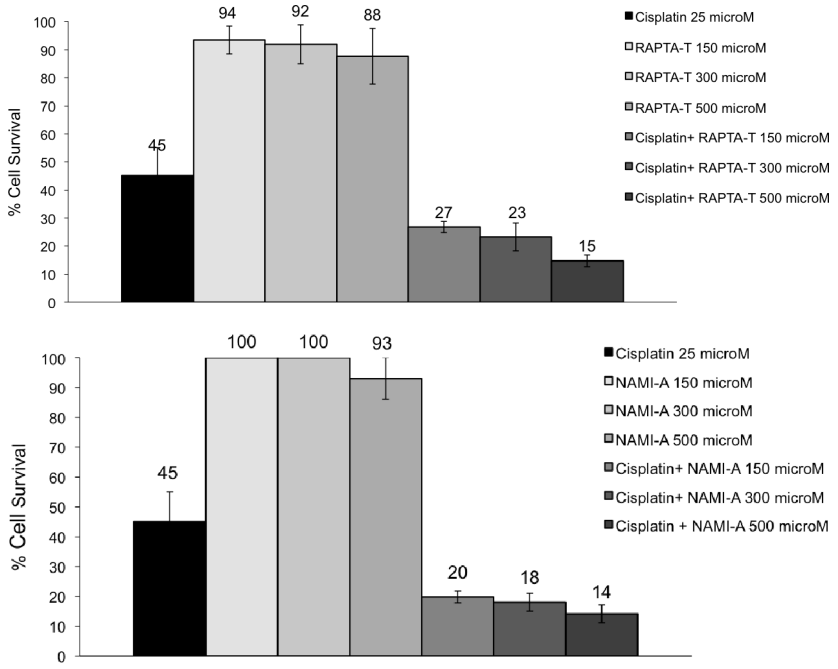

Figure 3. Survival of MCF7 cells subjected to 25 μM cisplatin and cisplatin with RAPTA-T (top) or NAMI-A (bottom) in combined treatments. Cell viability was measured on MCF7 cells after 72 h treatments using the MTT assay. Data are the mean ± SD of two experiments performed in eight replicate wells. Tukey−Kramer multiple comparison test: cisplatin + ruthenium compound $p < 0.01$ vs cisplatin in all cases.

Table 2. Comparison of the Expected Survival Rates (Based on an Assumption That the Combined Drug Activities Are Additive) and the Experimentally Determined Values after Treating Cells with Cisplatin and Different Concentrations of RAPTA-T or NAMI-A[a]

	survival rate					
	MCF7		A2780		A2780cisR	
combination	expected	observed	expected	observed	expected	observed
cisplatin + RAPTA-T 150 μM	0.42	0.27*	0.48	0.29*	0.54	0.25*
cisplatin + RAPTA-T 300 μM	0.41	0.23*	0.51	0.23*	0.47	0.18*
cisplatin + RAPTA-T 500 μM	0.40	0.15*	0.51	0.20*	0.40	0.20*
cisplatin + NAMI-A 150 μM	0.45	0.20*	0.39	0.32	0.43	0.32
cisplatin + NAMI-A 300 μM	0.45	0.18*	0.28	0.30	0.38	0.31
cisplatin + NAMI-A 500 μM	0.42	0.14*	0.14	0.23	0.23	0.27

[a] Cisplatin concentration was 25 μM (MCF7), 1 μM (A2780), or 10 μM (A2780cisR). Calculation of the predicted survival rates is described in the Experimental Section. The obtained values were statistically analyzed using a t-test (*$p < 0.05$).

A ca. 1.5- to 2-fold increase in cytotoxicity was observed at 150 μM RAPTA-T or NAMI-A and a ca. 2- to 2.4-fold increase at the maximum concentrations of the ruthenium compounds (see Table 2). All the observed survival rates for combinations of RAPTA-T at different concentrations with cisplatin indicate the occurrence of a synergistic effect. Conversely, NAMI-A treatment led to survival rates inferior to the ones expected from an additive effect only at 150 μM for both the cell lines.

To establish whether PARP-1 inhibition by the ruthenium compounds could contribute to the observed synergistic effects on MCF7 cells, PARP-1 activity was evaluated on protein extracts obtained from MCF7 cells pretreated with noncytotoxic doses of each compound. MCF7 cells were incubated with 150 μM RAPTA-T or NAMI-A or with 15 μM cisplatin for 72 h and the protein extracts collected and analyzed for PARP-1 activity. NAMI-A and RAPTA-T treatments inhibited PARP-1 by about 15% when administered at 150 μM. Notably, despite a 10-fold reduced dose with respect to the ruthenium complexes, cisplatin treatment resulted in PARP-1 activity being reduced by ca. 17% compared to the untreated cells. In contrast, in HT29 colon carcinoma cells, cisplatin treatment led to an increase in PARP-1 activity.[52] The difference between the cell lines is possibly due to a cisplatin resistant phenotype of these HT29 cells, carrying a p53 mutation.[52]

In order to study the influence of the compounds on PARP-1 expression induced by possible DNA damage, Western blot analysis was performed on protein extracts from MCF7 cells treated for 24 and 72 h with the same concentrations of ruthenium complexes and cisplatin as described above. For both NAMI-A- and RAPTA-T-treated samples, PARP-1 remained

dx.doi.org/10.1021/jm2000135 |J. Med. Chem. 2011, 54, 2196–2206

mainly in its intact form and the protein expression levels were essentially unaltered with respect to the controls (Figure 4), which supports the idea that the observed PARP-1 reduced activity in MCF7 protein extracts is due to direct enzyme inhibition by the ruthenium complexes. For cisplatin, marked apoptotic proteolysis of PARP-1 was detected after 24 h, as observed previously for other cell lines.[52]

PARP-1 inhibition by the complexes might be due to direct modification of the ZF domain of the protein. In fact, it has already been reported that modification of the zinc finger core by electrophilic agents results in inhibition of the nucleic acid binding capacity of the modified peptide.[53] Other studies describe the binding of platinum complexes to ZF structures.[54−56] Indeed, it has already been shown that cisplatin inhibits human DNA polymerase-α via covalent interactions with the cysteine residues of the ZF motif.[57−59] Recently, platinum-nucleobase complexes were reported to cause zinc displacement and loss of tertiary structure from the C-terminal ZF of retroviral proteins.[60,61] Gold complexes were also shown to efficiently react with ZFs with substitution by Au of the Zn ion, with the formation of so-called "gold fingers".[62,63] Indeed, a number of medicinally relevant gold-based compounds are known to alter essential ZF domains in proteins or model peptides with crucial biological function, including DNA binding proteins.[64]

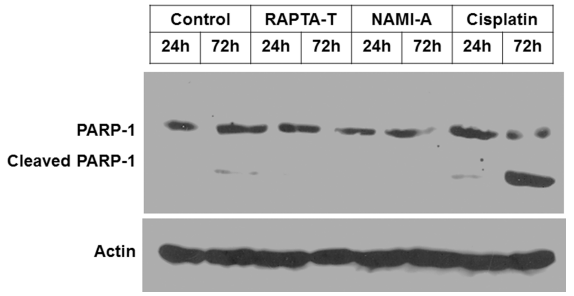

Figure 4. Western blot analysis of the expression of PARP-1 in MCF7 cells after incubation with RAPTA-T and NAMI-A (150 μM) and cisplatin (15 μM) for 24 and 72 h. Total cellular protein extracts (30 μg) were analyzed by Western blot with an anti-PARP-1 antibody. Controls consisted of samples of untreated cells. Actin was used as an internal loading control.

In order to establish the nature of PARP-1 inhibition by the complexes at a molecular level, e.g. whether inhibition involves coordination of the drugs to the zinc binding domain of the protein, substitution of the Zn ion, and binding stoichiometry, FT-ICR mass spectrometry was carried out using a peptide containing the N-terminal zinc finger domain of PARP-1, initially in the absence of Zn^{2+} (apo-ZF-PARP), with a complex-to-protein ratio of 3:1. This specific ZF-PARP domain was chosen as the N-terminus of the peptide and is essential for PARP-1 activation by double-stranded DNA breaks.[20]

Incubation of the complexes with the apo-ZF-PARP peptide (monoisotopic molecular mass 5116.46 Da) leads to the formation of new adducts. The extent of adduct formation (estimated from the peaks assigned to adducts relative to the unmodified apo-ZF-PARP) follows the trend: Aubipy ≈ Auphen ≫ NAMI-A > auranofin > cisplatin > RAPTA-T, which is in excellent agreement with the data obtained from the inhibition assays performed on the pure protein and MCF7 cell extracts. The Au(III) compounds, Aubipy and Auphen, which inhibit PARP-1 at nanomolar concentrations, show much higher reactivity than the other compounds, with extensive adduct formation taking place after only a few minutes (see Figure 5), with up to three bound Au ions detected. Notably, in the obtained spectra, apart from the peak of the apo-ZF-PARP peptide (m/z 732.3602 for the 7+ charge state), peaks corresponding to "naked" Au ions (in which all the original ligands are absent) bound to the peptide are observed at m/z 759.7792, m/z 787.9172, and m/z 816.0562 for one, two, and three Au ions bound to the ZF-PARP in the 7+ charge state, respectively. Isotope cluster analysis indicates that the first Au ion is in oxidation state +3, whereas additional gold ions have undergone reduction to the +1 state—note that redox processes are not uncommon for Au(III) complexes interacting with peptides.[65]

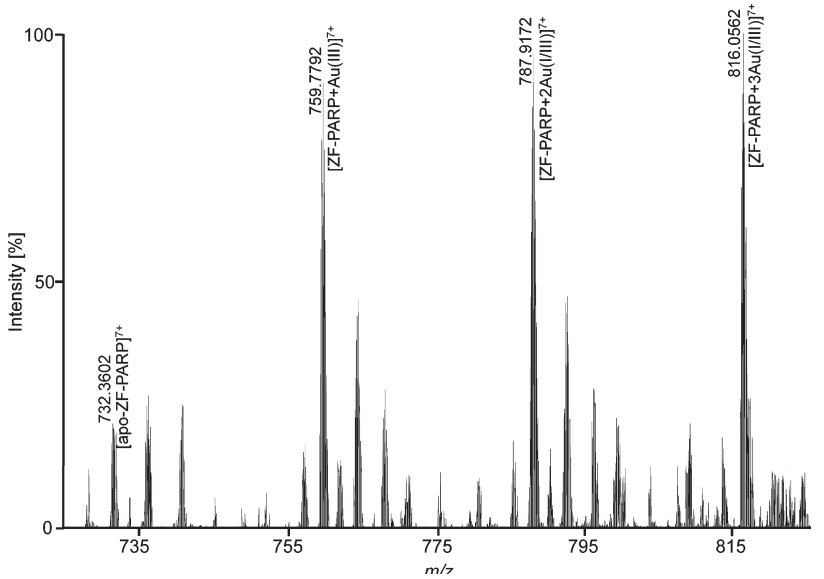

Figure 5. ESI FT-ICR MS of apo-ZF-PARP incubated with Aubipy in a 1:3 ratio for 15 min. The expanded segment of the mass spectrum in the range m/z 720−825 shows the adducts in the 7+ charge state. The m/z value for the most intense isotope of each gold-adduct peak is given. Unlabeled peaks correspond to adducts formed with ubiquitous sodium and potassium ions.

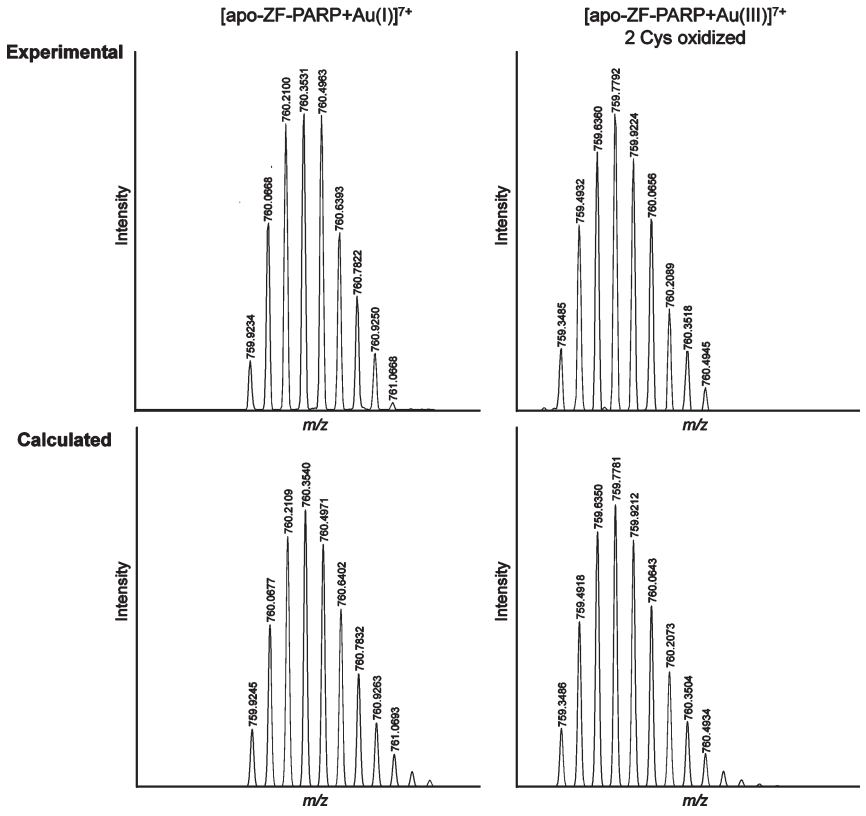

Figure 6. Comparison of adducts formed between apo-ZF-PARP and Au(I) (auranofin, top left) and Au(III) (Aubipy, top right) obtained with ESI FT-ICR MS with their corresponding calculated mass spectra (bottom).

Similar results were obtained with auranofin, with up to two Au ions bound to the ZF-PARP detected. Figure 6 depicts the expanded segments of the mass spectra around the 7+ charge state of an adduct formed between the zinc finger and auranofin (gold in the oxidation state +1) and Aubipy (gold in the oxidation state +3). As mentioned above, all the original ligands are lost from both compounds, leading to adducts of the type Au-ZF-PARP, which only incorporates the metal ion. Comparison of the experimentally and theoretically obtained isotopic patterns in the 7+ charge states shows that, in the case of auranofin, the gold ion remains in the +1 oxidation state. For Aubipy the signal of the adduct is shifted by m/z 0.5739, corresponding to approximately 4 Da at $z = 7$. This indicates not only that the gold remains in the oxidation state +3 (therefore requiring two protons less for ionization) but also that two additional cysteine residues are involved in the binding (leading to the replacement of the sulfur-bound hydrogens by the gold), which is in agreement with the expected square planar binding mode of Au(III) in comparison to the linear coordination geometry characteristic of Au(I).

In the case of RAPTA-T, the compound takes several hours for adducts to be observed. The toluene and PTA ligands remain attached to the ruthenium center upon binding to the protein, with only loss of the chlorides observed, which is in keeping with RAPTA compounds binding to proteins as observed by MS[66,67] and X-ray crystallography.[68] For NAMI-A, only the imidazole moiety remains attached to the ruthenium center upon adduct formation (adducts containing only the Ru ion are observed following prolonged incubation). Additionally, as already observed in DNA binding studies,[69] a series of aquated species are detected for the Ru(III) compound, complicating data analysis due to the large number of possible combinations.

In the case of cisplatin, the major adducts formed (Figure 7) correspond to a "naked" platinum(II) ion (e.g., peak at m/z 759.9225 in Figure 7), although peaks of low relative intensity, corresponding to binding of a $Pt(NH_3)^{2+}$ moiety, are also observed (e.g., the peaks centered at m/z 762.2092 in Figure 7).

The apo-ZF-PARP was incubated with zinc acetate in order to create the physiological ZF-motif (holo-ZF-PARP). The zinc salt was added to the apo-ZF-PARP before the metal complexes to ascertain whether the metallodrugs are able to displace coordinated zinc. In another series of experiments, the zinc salt and metal complexes were added simultaneously to mimic competitive binding conditions. ZF-PARP preincubated with the metallodrugs was also treated with the zinc salt to determine whether Zn(II) can displace the metallodrugs and to establish whether Zn(II) and other metal ions bind to the same residues.

For the Au(III) compounds, the spectra obtained are comparable in all three experimental setups: within minutes an equilibrium between the Zn- and Au-bound species is established, evidenced, for example, by peaks at m/z 1296.6061 and m/z 1329.8654 for the Zn(II) and Au(III) bound 4+ charged species, respectively (Figure 8, top). Although the spectra are not quantitative, the ratio of Au- to Zn-bound ZF-PARP is approximately 3:1, indicating a higher binding affinity of the thiophilic Au ion compared to the Zn ion toward the ZF motif. These results also suggest that the Zn and Au ions compete for the same binding site on the ZF-PARP and provide evidence that direct disruption of zinc finger function may represent a mechanism for the highly efficient inhibition of PARP-1 activity. Moreover, due to the competition with the Zn ion, and at variance with the apo-ZF-PARP data, only gold monoadducts were observed. A peak containing both Au and Zn ions bound to the

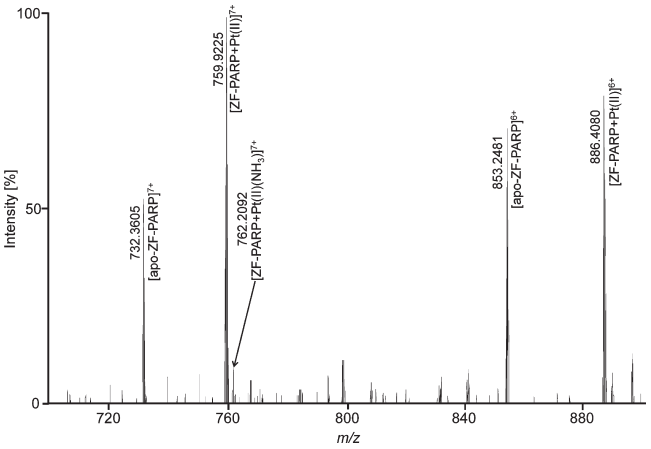

Figure 7. ESI FT-ICR MS of apo-ZF-PARP incubated with cisplatin for 24 h. The expanded segment of the mass spectrum in the range m/z 700−900 shows the 7+ and 6+ charge states. The m/z value for the most intense isotope of major peaks is given.

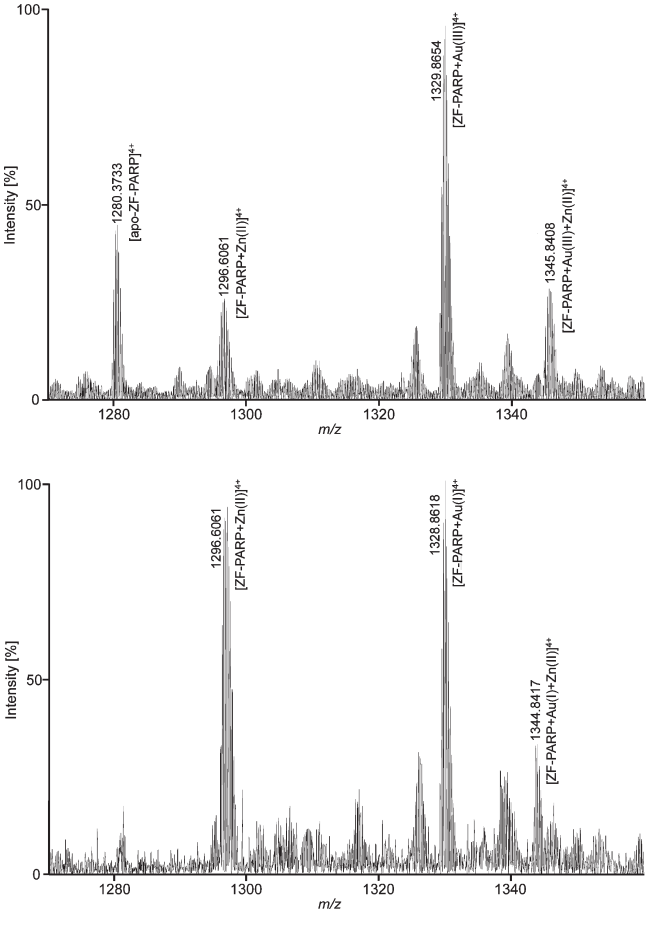

Figure 8. ESI FT-ICR MS of (top) apo-ZF-PARP with zinc acetate and Aubipy in a 1:2:2 ratio incubated for 10 min under competitive conditions, and (bottom) of apo-ZF-PARP preincubated with zinc acetate and subsequent addition of auranofin (24 h) in a 1:2:2 ratio. The m/z value of the most intense isotope of each peak is given. Unlabeled peaks correspond to adducts formed with ubiquitous sodium and potassium ions.

ZF-PARP is observed (m/z 1345.8408 in Figure 8 for the 4+ charge state), indicating that additional residues might also serve as binding sites for the metal ions once the ZF motif is saturated.

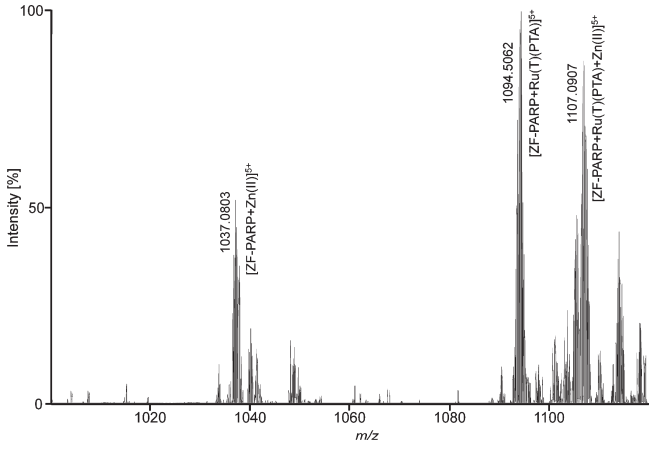

Figure 9. ESI FT-ICR MS of apo-ZF-PARP preincubated with zinc acetate and subsequent addition of RAPTA-T (24 h) in a 1:2:2 ratio. The m/z value for the most intense isotope of each peak is given. Unlabeled peaks correspond to adducts formed with ubiquitous sodium and potassium ions.

In the case of auranofin (Figure 8, bottom), competition between the Zn(II) and Au(I) ions for the zinc binding motif is also observed. The ratio between the two species at equilibrium may be estimated to be only 1:1 (Figure 8; peaks at m/z 1296.6061 and m/z 1328.8618, respectively), thereby confirming results obtained with the apo-ZF-PARP, which also showed more efficient adduct formation between the peptide and Au(III) compared to Au(I) ions. Again, a minor peak is observed that may be attributed to a species containing both zinc and gold ions (m/z 1344.8417). The lower reactivity of auranofin relative to the Au(III) complexes is also in excellent agreement with the lower IC_{50} value observed in the PARP-1 inhibition studies (ca. by 1 order of magnitude).

Addition of RAPTA-T to the Zn(II)-ZF-PARP results in peaks corresponding to binding of compound via loss of two chloride ligands, in addition to the Zn(II) ion (peaks at m/z 1094.5062 and m/z 1037.0803, respectively, in Figure 9), as observed for the apo-ZF-PARP. As highly abundant species contain both Zn(II) and the RAPTA-T fragment (e.g., peak centered at m/z 1107.0907 in Figure 9), it is not unreasonable that the Ru-adduct coordinates to amino acids other than those of the zinc finger motif. This is not surprising, as Ru(II)-arene adducts have been shown to be able to coordinate to aspartate carboxylate O atoms, the hydroxyl functions of serine, and the amino N atoms of lysine residues,[70] all of which are also present in the ZF-PARP peptide. Such secondary interactions are likely to interfere with the activity of the enzyme to a lesser extent, which is consistent with the lower inhibitory effect of RAPTA-T.

NAMI-A forms the same ensemble of adducts with the zinc-modified peptide as in the experiments with the apo-ZF-PARP (i.e., "naked" Ru, Ru-imidazole, and a series of aquated species, depending on the incubation time) (Figure 10), and no species with bound zinc are observed. Apparently, the multidentate binding mode of the NAMI-A fragments blocks the ZF motif directly or interferes strongly with the secondary structure of the protein, preventing Zn(II) ions from binding to the peptide. These observations correlate well with the rather high activity of NAMI-A in the PARP-1 inhibition assay on MCF7 cell extracts.

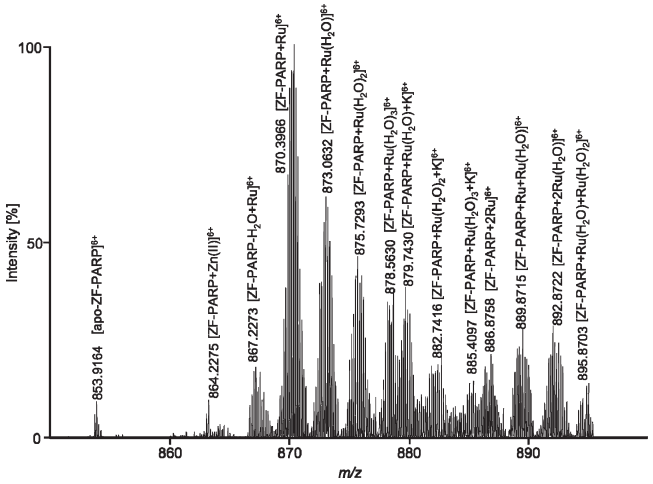

Figure 10. ESI FT-ICR MS of apo-ZF-PARP preincubated with zinc acetate and subsequent addition of NAMI-A (24 h) in a 1:2:2 ratio. The m/z value for the most intense isotope of each peak is given. Unlabeled peaks correspond to adducts formed with ubiquitous sodium and potassium ions.

The spectra obtained upon incubation of the Zn(II)-ZF-PARP with cisplatin give peaks that may be assigned to adducts of Pt^{2+} or $Pt(NH_3)^{2+}$ containing species (as for the apo-ZF-PARP) and indicate direct competition with the Zn(II) ion for the zinc binding motif (1:1 Pt:Zn adduct formation). Peaks of very low abundance show concomitant coordination of both Pt and Zn.

CONCLUSIONS

A series of anticancer metal complexes were found to inhibit PARP-1 activity more efficiently than the benchmark inhibitor 3-AB; the extent of inhibition follows the trend Au(III) > Au(I) > Pt(II) > Ru(III) > Ru(II) > 3-AB. Enzyme activity assays performed on purified PARP-1, and on protein extracts from cancer cells, show differences, that presumably correspond to the reactivity of the complexes with other proteins/enzymes in the cell extracts. It should be noted, however, that cisplatin inhibits PARP-1 to the same extent as 3-AB in cell extracts, and this feature should not be excluded when considering the overall pharmacological profile of this widely used anticancer drug. Moreover, for clinically used gold-based drugs, PARP-1 or more generally ZF proteins appear to be relevant targets.

The ruthenium complexes (at noncytotoxic doses) were coadministered with cisplatin, resulting in a synergic increase in cytotoxicity in the case of MCF7 cells treated with either RAPTA-T or NAMI-A. This effect is likely to correspond to a reduced repair of the platinated DNA adducts due to (partial) PARP-1 inhibition by the ruthenium complexes, although other mechanisms cannot be excluded. Notably, treatment with the ruthenium compounds did not affect PARP-1 expression, as confirmed by Western blot analysis. In the case of A2780 and A2780cisR cells, only RAPTA-T demonstrated a synergistic effect. Although caution should be taken in transferring the results of *in vitro* models to the *in vivo* reality, the observed effects provide further evidence that ruthenium compounds act via a different mechanism of action with respect to the DNA damage induced by cisplatin, as indicated in an *in vivo* combination study using cisplatin and NAMI-A, which demonstrated the compatibility of the concomitant treatment of malignant carcinomas with two metal-based drugs.[71]

Excellent correlation between PARP-1 inhibition in protein extracts and the mode of metal binding was observed. The gold(III)-based compounds rapidly lose all their ligands upon binding to the zinc finger domain, which presumably results in tetradentate binding through 1 His and 3 Cys residues. Similar behavior is observed for cisplatin, whereas the ruthenium compound RAPTA-T only loses the two chloride ligands. For NAMI-A, a series of possible adducts is observed, including loss of all original ligands and species containing the imidazole and/or aqua moieties. Notably, all compounds were able to compete with Zn(II) for the binding site in the ZF-PARP to some extent; the Au(III) compounds, which showed the highest inhibitory potencies, were most efficient in this regard. The high reactivity of gold(III) complexes toward ZF peptides with respect to platinum(II) compounds is in accordance with previous studies.[63]

EXPERIMENTAL SECTION

Materials and Reagents. RAPTA-T,[72] NAMI-A,[73] Auphen,[44] and Aubipy[46] were prepared according to literature methods. Their purity was confirmed by ESI MS, ^{1}H NMR spectroscopy, and elemental analysis. Cisplatin was purchased from Sigma-Aldrich and auranofin from Alexis Biochemicals. The PARP-1 zinc binding domain (GRASCKKCSESIPKDSLRMAIMVQSPMFDGKVPHWYHFSCFWKV) was purchased from Peptide Specialty Laboratories GmbH (Heidelberg, Germany). Dithiothreitol (DTT; molecular biology grade) and zinc acetate dihydrate (p.a.) were obtained from Sigma-Aldrich.

Cell Culture. The human breast cancer cell line MCF7 and human ovarian cancer cell lines A2780 and A2780cisR (resistant to cisplatin) were cultured respectively in DMEM (Dulbecco's Modified Eagle Medium) and RPMI containing GlutaMaxI supplemented with 10% FBS and 1% penicillin/streptomycin (all from Invitrogen), at 37 °C in a humidified atmosphere of 95% of air and 5% CO_2 (Heraeus, Germany). Where indicated, MCF7 cells were grown for 72 h prior to the assays in DMEM containing GlutaMaxI supplemented with 1% or 3% of FBS.

Cell Growth Inhibition. Cell viability was evaluated by using a colorimetric method based on the tetrazolium salt MTT [3-(4,5-dimethylthiazol-2-yl)-2,5-diphenyltetrazolium bromide], which is reduced by viable cells to yield purple formazan crystals. Cells were seeded in 96-well plates at a density of $(8-15) \times 10^3$ cells per well (200 μL). After overnight attachment, the medium was replaced by 200 μL of a dilution series of the compounds in the medium, and cells were incubated for a further 72 h. Stock solutions of the complexes were prepared in water for cisplatin and the ruthenium compounds, auranofin was dissolved in EtOH and Aupiby and Auphen in DMSO. The percentage of DMSO or ethanol in the culture medium did not exceed 0.2%. At the end of the 72 h incubation period, the media was removed and the cells were incubated with MTT (0.5 mg/mL in culture medium; 200 μL) for 3−4 h at 37 °C and 5% CO_2. The purple formazan crystals formed inside the cells were then dissolved in 200 μL of DMSO by thorough shaking, and the absorbance was read at 570 nm, using a plate spectrophotometer (Power Wave Xs; Bio-Tek). Each test was performed with at least six replicates and repeated at least 2 times. The IC_{50} value is expressed as percentage of the surviving cells in relation with the control (cells with regular medium).

Additive and Synergistic Cytotoxicity Analysis. The combination index method of Chou and Talaly was used to determine whether the observed interactions between cisplatin and the ruthenium drugs were additive or synergistic.[51] If the interaction was additive, the sum of the effects of the two drugs should be equal to the product of their fractional activities. The representative function defined as the expected cell survival rate corresponds to $f(u)1,2 = f(u)1 \cdot f(u)2$, where $f(u)1$ = the

fraction unaffected by drug 1, $f(u)2$ = the fraction unaffected by drug 2, and $f(u)1,2$ = the fraction unaffected by drugs 1 and 2.[74] The expected and observed cell survival rates obtained from a minimum of six replicates and of at least three repetitions were analyzed by the Student's t test (p); $p < 0.05$ was viewed as significant.

Preparation of Cell Extracts. MCF7 cells were grown in DMEM GlutaMaxI with 10% FBS (or 3% and 1% when indicated) and incubated with different doses of the compounds. After 72 h, cells were scraped in ice-cold PBS and centrifuged at 10000*g* for 10 s at 4 °C. The pellet was resuspended in 5−10 volumes of lysis buffer (PARP Buffer, Trevigen) containing complete protease inhibitor cocktail tablets (Roche), 0.4 M NaCl, and 1% Triton X-100). After 15 min on ice, lysates were centrifuged at 14000*g* for 10 min at 4 °C to pellet the cellular debris and the supernatants were removed for further use. The total protein content was determined by using the DC Protein Assay Kit (Biorad).

PARP-1 Activity Determinations. PARP-1 activity was determined using Trevigen's HT Universal Colorimetric PARP Assay. This assay measures the incorporation of biotinylated poly(ADP-ribose) onto histone proteins in a 96 microtiter strip well format. Either recombinant human PARP-1 (high specific activity, purified from *E.coli* containing recombinant plasmid harboring the human PARP gene, supplied with the assay kit) or an aliquot of protein cell extracts (50 μg) was used as the enzyme source. 3-Aminobenzamide (3-AB), provided in the kit, was used as control inhibitor. Two controls were always performed in parallel: a positive activity control for PARP-1 without inhibitors, that provided the 100% activity reference point, and a negative control, without PARP-1 to determine background absorbance. The final reaction mixture (50 μL) was treated with TACS-Sapphire, a horseradish peroxidase colorimetric substrate, and incubated in the dark for 30 min. Absorbance was read at 630 nm after 30 min. The data correspond to the mean of at least three experiments performed in triplicate ± SD.

Evaluation of PARP-1 Expression by Western Blot Analysis. MCF7 cells were incubated for 24 or 72 h with 150 μM of RAPTA-T or NAMI-A or 15 μM of cisplatin and then lysed in Cell Lytic-MT Extraction reagent (Sigma) supplemented with Complete protease inhibitor cocktail tablets (Roche Applied Science). After 15 min on ice, lysates were centrifuged at 14000*g* for 10 min at 4 °C to pellet the cellular debris, and the supernatants were removed for further use. The total protein content was determined by using the DC Protein Assay Kit (Biorad), and aliquots of protein (30 μg) from each sample were analyzed using standard Western blot procedures. Briefly, protein extracts were subjected to electrophoresis on a 7% SDS-polyacrylamide gel and transferred electrophoretically onto nitrocellulose membranes. The blots were blocked with PBS-T containing 5% nonfat dry milk for 1 h. The blotting membranes were incubated with primary antibodies against PARP-1 (1:1000, Cell Signaling) and actin (1:8000, Sigma) overnight. Membranes were washed with PBS-T and incubated for 1 h with secondary antibodies (anti-mouse IgG-HRP and goat anti-rabbit IgG-HRP, Biorad) diluted 1:3000. Finally, membranes were developed using the SuperSignal WetsPico Substrate kit (Pierce, Rockford, IL) according to the manufacturer's instructions.

Mass Spectrometry. Samples comprising 50 μM ZF-PARP-peptide (pretreated with 3 equiv of DTT to ensure reduced cysteine residues) and 150 μM of the corresponding complex were prepared in ammonium carbonate buffer (10 mM, pH 7.4) and incubated for up to 24 h at 37 °C prior to analysis. For Zn displacement experiments, the reduced ZF-PARP-peptide was incubated with zinc acetate in a ratio of 1:3 for 15 min prior to addition of the metallodrug. Quantitative binding of the zinc ion was confirmed by label-free ESI MS. The samples were diluted 10-fold with HPLC MS purity grade water before measurement and analyzed in positive ion mode using a hyphenated ion trap-FT-ICR mass spectrometer comprising an LTQ XL and a 12 T FT-ICR MS (both ThermoFisher Scientific, Bremen, Germany) at a resolution of 25000 at 400 m/z specified for a 7 T magnetic field, described elsewhere.[75,76] Samples were introduced by direct infusion either with a standard ESI ion source at a rate of 4 μL/min or using an Advion TriVersa nano-ESI robot (Advion Biosciences, Ithaca, NY, USA) equipped with a 5.5 μm-nozzle chip, providing a flow rate of ~300 nL/min. The ESI robot was controlled with ChipSoft v7.2.0 software employing a gas pressure of 0.45 psi and a voltage of 1.7 kV. The Xcalibur software bundle (ThermoFisher Scientific) was utilized for data acquisition and data analysis.

AUTHOR INFORMATION

Corresponding Author
*Phone: +41 21 6939860. E-mail: angela.casini@epfl.ch.

ACKNOWLEDGMENT

We thank the EPFL, Swiss National Science Foundation (SNSF) (AMBIZIONE Project No. PZ00P2-121933/1), the Swiss Confederation (Action COST D39—Accord de recherche—SER Project No. C09.0027), and COST D39 for financial support. M.G. thanks the Austrian Science Foundation for financial support (Schrödinger Fellowship J2882-N19). Y.O. T. thanks the SNSF (Project 200021-125147/1) for the partial financial support of the ESI FT-ICR MS operational costs.

ABBREVIATIONS USED

ADP, adenosine diphosphate; Bipy, 2,2′-bipyridine; DMEM, Dulbecco's Modified Eagle Medium; dmso, methyl sulfoxide; DTT, dithiothreitol; ESI MS, electrospray ionization mass spectrometry; FBS, fetal bovine serum; FT-ICR MS, Fourier transform ion cyclotron resonance mass spectrometry; Him, imidazole; MTT, 3-(4,5-dimethylthiazol-2-yl)-2,5-diphenyltetrazolium bromide; PARP, poly(adenosine diphosphate ribose) polymerase; PBS, phosphate buffered saline; Phen, 1,10-phenatroline; PTA, 1,3,5-triaza-7-phosphaadamantane; ZF, zinc-finger

REFERENCES

(1) Rosenberg, B.; Vancamp, L.; Krigas, T. Inhibition of Cell Division in Escherichia Coli by Electrolysis Products from a Platinum Electrode. *Nature* **1965**, *205*, 698–699.

(2) Barnes, K. R.; Lippard, S. J. Cisplatin and related anticancer drugs: Recent advances and insights. *Metal Ions in Biolgical Systems, Vol 42: Metal Complexes in Tumor Diagnosis and as Anticancer Agents* **2004**, No. 42, 143–177.

(3) Jakupec, M. A.; Galanski, M.; Arion, V. B.; Hartinger, C. G.; Keppler, B. K. Antitumour metal compounds: more than theme and variations. *Dalton Trans.* **2008**, 183–194.

(4) Clarke, M. J.; Zhu, F. C.; Frasca, D. R. Non-platinum chemotherapeutic metallopharmaceuticals. *Chem. Rev.* **1999**, *99*, 2511–2533.

(5) Kostova, I. Ruthenium complexes as anticancer agents. *Curr. Med. Chem.* **2006**, *13*, 1085–1107.

(6) Reedijk, J. Platinum Anticancer Coordination Compounds: Study of DNA Binding Inspires New Drug Design. *Eur. J. Inorg. Chem.* **2009**, 1303–1312.

(7) Aris, S. M.; Farrell, N. P. Towards Antitumor Active trans-Platinum Compounds. *Eur. J. Inorg. Chem.* **2009**, 1293–1302.

(8) Hanigan, M. H.; Devarajan, P. Cisplatin nephrotoxicity: molecular mechanisms. *Cancer Therapy* **2003**, *1*, 47–61.

(9) Wang, D.; Lippard, S. J. Cellular processing of platinum anticancer drugs. *Nature Rev. Drug Discovery* **2005**, *4*, 307–320.

(10) Dyson, P. J.; Sava, G. Metal-based antitumour drugs in the post genomic era. *Dalton Ttans.* **2006**, 1929–1933.

(11) Timerbaev, A. R.; Hartinger, C. G.; Aleksenko, S. S.; Keppler, B. K. Interactions of antitumor metallodrugs with serum proteins: Advances in characterization using modern analytical methodology. *Chem. Rev.* **2006**, *106*, 2224–2248.

(12) Casini, A.; Gabbiani, C.; Sorrentino, F.; Rigobello, M. P.; Bindoli, A.; Geldbach, T. J.; Marrone, A.; Re, N.; Hartinger, C. G.; Dyson, P. J.; Messori, L. Emerging Protein Targets for Anticancer Metallodrugs: Inhibition of Thioredoxin Reductase and Cathepsin B by Antitumor Ruthenium (II)-Arene Compounds. *J. Med. Chem.* **2008**, *51*, 6773–6781.

(13) Casini, A.; Edafe, F.; Erlandsson, M.; Gonsalvi, L.; Ciancetta, A.; Re, N.; Ienco, A.; Messori, L.; Peruzzini, M.; Dyson, P. J. Rationalization of the inhibition activity of structurally related organometallic compounds against the drug target cathepsin B by DFT. *Dalton Trans.* **2010**, *39*, 5556–5563.

(14) Bindoli, A.; Rigobello, M. P.; Scutari, G.; Gabbiani, C.; Casini, A.; Messori, L. Thioredoxin reductase: A target for gold compounds acting as potential anticancer drugs. *Coord. Chem. Rev.* **2009**, *253*, 1692–1707.

(15) Milacic, V.; Fregona, D.; Dou, Q. P. Gold complexes as prospective metal-based anticancer drugs. *Histol. Histopathol.* **2008**, *23*, 101–108.

(16) Schreiber, V.; Dantzer, F.; Ame, J. C.; de Murcia, G. Poly(ADP-ribose): novel functions for an old molecule. *Nat. Rev. Mol. Cell Biol.* **2006**, *7*, 517–528.

(17) Jeggo, P. A. DNA repair: PARP—another guardian angel? *Curr. Biol.* **1997**, *8*, R49–R51.

(18) Nguewa, P. A.; Fuertes, M. A.; Valladares, B.; Alonso, C.; Perez, J. M. Poly(ADP-Ribose) polymerases: Homology, structural domains and functions. Novel therapeutical applications. *Prog. Biophys. Mol. Biol.* **2005**, *88*, 143–172.

(19) Demurcia, G.; Menissier, J. Poly(Adp-Ribose) Polymerase—A Molecular Nick-Sensor (Vol. *19*, Pg 172, **1994**). *Trends Biochem. Sci.* **1994**, *19*, 250−250.

(20) Ikejima, M.; Noguchi, S.; Yamashita, R.; Ogura, T.; Sugimura, T.; Gill, D. M.; Miwa, M. The Zinc Fingers of Human Poly(Adp-Ribose) Polymerase Are Differentially Required for the Recognition of DNA Breaks and Nicks and the Consequent Enzyme Activation—Other Structures Recognize Intact DNA. *J. Biol. Chem.* **1990**, *265*, 21907–21913.

(21) Kim, M. Y.; Zhang, T.; Kraus, W. L. Poly(ADP-ribosyl)ation by PARP-1: 'PAR-laying' NAD(+) into a nuclear signal. *Genes Dev.* **2005**, *19*, 1951–1967.

(22) Homburg, S.; Visochek, L.; Moran, N.; Dantzer, F.; Priel, E.; Asculai, E.; Schwartz, D.; Rotter, V.; Dekel, N.; Cohen-Armon, M. A fast signal-induced activation of poly(ADP-ribose) polymerase: A novel downstream target of phospholipase C. *J. Cell Biol.* **2000**, *150*, 293–307.

(23) Herceg, Z.; Wang, Z. Q. Functions of poly(ADP-ribose) polymerase (PARP) in DNA repair, genomic integrity and cell death. *Mutation Research-Fundamental and Molecular Mechanisms of Mutagenesis* **2001**, *477*, 97–110.

(24) Amaravadi, R. K.; Thompson, C. B. The roles of therapy-induced autophagy and necrosis in cancer treatment. *Clin. Cancer Res.* **2007**, *12*, 7271–7279.

(25) Lord, C. J.; Ashworth, A. Targeted therapy for cancer using PARP inhibitors. *Curr. Opin. Pharmacol.* **2008**, *8*, 363–369.

(26) Miknyoczki, S. J.; Jones-Bolin, S.; Pritchard, S.; Hunter, K.; Zhao, H.; Wan, W. H.; Ator, M.; Bihovsky, R.; Hudkins, R.; Chatterjee, S.; Klein-Szanto, A.; Dionne, C.; Ruggeri, B. Chemopotentiation of Temozolomide, irinotecan, and cisplatin activity by CEP-6800, a poly(ADP-ribose) polymerase inhibitor. *Mol. Cancer Therapeutics* **2003**, *2*, 371–382.

(27) Rottenberg, S.; Jaspers, J. E.; Kersbergen, A.; van der Burg, E.; Nygren, A. O. H.; Zander, S. A. L.; Derksen, P. W. B.; de Bruin, M.; Zevenhoven, J.; Lau, A.; Boulter, R.; Cranston, A.; O'Connor, M. J.; Martin, N. M. B.; Borst, P.; Jonkers, J. High sensitivity of BRCA1-deficient mammary tumors to the PARP inhibitor AZD2281 alone and in combination with platinum drugs. *Proc. Natl. Acad. Sci. U.S.A.* **2008**, *105*, 17079–17084.

(28) Evers, B.; Drost, R.; Schut, E.; de Bruin, M.; van der Burg, E.; Derksen, P. W. B.; Holstege, H.; Liu, X. L.; van Drunen, E.; Beverloo, H. B.; Smith, G. C. M.; Martin, N. M. B.; Lau, A.; O'Connor, M. J.; Jonkers, J. Selective inhibition of BRCA2-deficient mammary tumor cell growth by AZD2281 and cisplatin. *Clin. Cancer Res.* **2008**, *14*, 3916–3925.

(29) Donawho, C. K.; Luo, Y.; Luo, Y. P.; Penning, T. D.; Bauch, J. L.; Bouska, J. J.; Bontcheva-Diaz, V. D.; Cox, B. F.; DeWeese, T. L.; Dillehay, L. E.; Ferguson, D. C.; Ghoreishi-Haack, N. S.; Grimm, D. R.; Guan, R.; Han, E. K.; Holley-Shanks, R. R.; Hristov, B.; Idler, K. B.; Jarvis, K.; Johnson, E. F.; Kleinberg, L. R.; Klinghofer, V.; Lasko, L. M.; Liu, X. S.; Marsh, K. C.; McGonigal, T. P.; Meulbroek, J. A.; Olson, A. M.; Palma, J. P.; Rodriguez, L. E.; Shi, Y.; Stavropoulos, J. A.; Tsurutani, A. C.; Zhu, G. D.; Rosenberg, S. H.; Giranda, V. L.; Frost, D. J. ABT-888, an orally active poly(ADP-ribose) polymerase inhibitor that potentiates DNA-damaging agents in preclinical tumor models. *Clin. Cancer Res.* **2007**, *13*, 2728–2737.

(30) Helleday, T.; Petermann, E.; Lundin, C.; Hodgson, B.; Sharma, R. A. DNA repair pathways as targets for cancer therapy. *Nat. Rev. Cancer* **2008**, *8*, 193–204.

(31) Zhu, G. Y.; Lippard, S. J. Photoaffinity Labeling Reveals Nuclear Proteins That Uniquely Recognize Cisplatin-DNA Interstrand Cross-Links. *Biochemistry* **2009**, *48*, 4916–4925.

(32) Guggenheim, E. R.; Xu, D.; Zhang, C. X.; Chang, P. V.; Lippard, S. J. Photoaffinity Isolation and Identification of Proteins in Cancer Cell Extracts that Bind to Platinum-Modified DNA. *ChemBioChem* **2009**, *10*, 141–157.

(33) Guggenheim, E. R.; Ondrus, A. E.; Movassaghi, M.; Lippard, S. J. Poly(ADP-ribose) polymerase-1 activity facilitates the dissociation of nuclear proteins from platinum-modified DNA. *Bioorg. Med. Chem.* **2008**, *16*, 10121–10128.

(34) Zhang, C. X.; Chang, P. V.; Lippard, S. J. Identification of nuclear proteins that interact with platinum-modified DNA by photoaffinity labeling. *J. Am. Chem. Soc.* **2004**, *126*, 6536–6537.

(35) Zhu, G. Y.; Chang, P.; Lippard, S. J. Recognition of Platinum-DNA Damage by Poly(ADP-ribose) Polymerase-1. *Biochemistry* **2010**, *49*, 6177–6183.

(36) Curtin, N. J. PARP inhibitors for cancer therapy. *Expert Rev. Mol. Med.* **2005**, *7*, 1–20.

(37) Allardyce, C. S.; Dyson, P. J.; Ellis, D. J.; Heath, S. L. [Ru(eta(6)-p-cymene)Cl-2(pta)] (pta=1,3,5-triaza-7-phosphatricyclo-[3.3.1.1]decane): a water soluble compound that exhibits pH dependent DNA binding providing selectivity for diseased cells. *Chem. Commun.* **2001**, 1396–1397.

(38) Ang, W. H.; Dyson, P. J. Classical and non-classical ruthenium-based anticancer drugs: Towards targeted chemotherapy. *Eur. J. Inorg. Chem.* **2006**, 4003–4018.

(39) Bergamo, A.; Masi, A.; Dyson, P. J.; Sava, G. Modulation of the metastatic progression of breast cancer with an organometallic ruthenium compound. *Int. J. Oncol.* **2008**, *33*, 1281–1289.

(40) Alessio, E.; Mestroni, G.; Bergamo, A.; Sava, G. Ruthenium antimetastatic agents. *Curr. Top. Med. Chem.* **2004**, *4*, 1525–1535.

(41) Gianferrara, T.; Bratsos, I.; Alessio, E. A categorization of metal anticancer compounds based on their mode of action. *Dalton Trans.* **2009**, *37*, 7588–7598.

(42) Kean, W. F.; Hart, L.; Buchman, W. W. Auranofin. *Br. J. Rheumatol.* **1997**, *36*, 560–572.

(43) Nobili, S.; Mini, E.; Landini, I.; Gabbiani, C.; Casini, A.; Messori, L. Gold Compounds as Anticancer Agents: Chemistry, Cellular Pharmacology, and Preclinical Studies. *Med. Res. Rev.* **2010**, *30*, 550–580.

(44) Messori, L.; Abbate, F.; Marcon, G.; Orioli, P.; Fontani, M.; Mini, E.; Mazzei, T.; Carotti, S.; O'Connell, T.; Zanello, P. Gold(III) complexes as potential antitumor agents: Solution chemistry and cytotoxic properties of some selected gold(III) compounds. *J. Med. Chem.* **2000**, *43*, 3541–3548.

(45) Abbate, F.; Orioli, P.; Bruni, B.; Marcon, G.; Messori, L. Crystal structure and solution chemistry of the cytotoxic complex 2,2-dichloro-(o-phenantroline)gold(III) chloride. *Inorg. Chim. Acta* **2000**, 311.

(46) Marcon, G.; Carotti, S.; Coronnello, M.; Messori, L.; Mini, E.; Orioli, P.; Mazzei, T.; Cinellu, M. A.; Minghetti, G. Gold(III) complexes with bipyridyl ligands: Solution chemistry, cytotoxicity, and DNA binding properties. *J. Med. Chem.* **2002**, *45*, 1672–1677.

(47) Nguewa, P. A.; Fuertes, M. A.; Cepeda, V.; Alonso, C.; Quevedo, C.; Soto, M.; Perez, J. M. Poly(ADP-ribose) Polymerase-1 Inhibitor 3-Aminobenzamide Enhances Apoptosis Induction by Platinum Complexes in Cisplatin-Resistant Tumor Cells. *Med. Chem.* **2006**, 2.

(48) Antonarakis, E. S.; Emadi, A. Ruthenium-based chemotherapeutics: are they ready for prime time? *Cancer Chemother. Pharm.* **2010**, *66*, 1–9.

(49) Frausin, F.; Cocchietto, M.; Bergamo, A.; Searcia, V.; Furlani, A.; Sava, G. Tumour cell uptake of the metastasis inhibitor ruthenium complex NAMI-A and its in vitro effects on KB cells. *Cancer Chemother. Pharm.* **2002**, *50*, 405–411.

(50) Liu, M. M.; Lim, Z. J.; Gwee, Y. Y.; Levina, A.; Lay, P. A. Characterization of a Ruthenium(III)/NAMI-A Adduct with Bovine Serum Albumin that Exhibits a High Anti-Metastatic Activity. *Angew Chem., Int. Ed.* **2010**, *49*, 1661–1664.

(51) Chou, T. C.; Talalay, P. Quantitative-Analysis of Dose-Effect Relationships—the Combined Effects of Multiple-Drugs or Enzyme-Inhibitors. *Adv. Enzyme Regulation* **1984**, *22*, 27–55.

(52) Gambi, N.; Tramontano, F.; Quesada, P. Poly(ADPR)-potymerase inhibition and apoptosis induction in cDDP-treated human carcinoma cell lines. *Biochem. Pharmacol.* **2008**, *75*, 2356–2363.

(53) Witkiewicz-Kucharczyk, A.; Bal, W. Damage of zinc fingers in DNA repair proteins, a novel molecular mechanism in carcinogenesis. *Toxicol. Lett.* **2006**, *162*, 29–42.

(54) Almaraz, E.; de Paula, Q. A.; Liu, Q.; Reibenspies, J. H.; Darensbourg, M. Y.; Farrell, N. P. Thiolate bridging and metal exchange in adducts of a zinc finger model and Pt-II complexes: Biomimetic studies of protein/Pt/DNA interactions. *J. Am. Chem. Soc.* **2008**, *130*, 6272–6280.

(55) Bose, R. N.; Yang, W. W.; Evanics, F. Structural perturbation of a C4 zinc-finger module by cis-diamminedichloroplatinum(II): insights into the inhibition of transcription processes by the antitumor drug. *Inorg. Chim. Acta* **2005**, *358*, 2844–2854.

(56) Liu, Q.; Golden, M.; Darensbourg, M. Y.; Farrell, N. Thiolate-bridged heterodinuclear platinum-zinc chelates as models for ternary platinum-DNA-protein complexes and zinc ejection from zinc fingers. Evidence from studies using ESI-mass spectrometry. *Chem. Commun.* **2005**, 4360–4362.

(57) Kelley, T. J.; Moghaddas, S.; Bose, R.; Basu, S. Inhibition of Immunopurified DNA Polymerase-Alpha from Pa-3 Prostate Tumor-Cells by Platinum (II) Antitumor Drugs. *Cancer Biochem. Biophys.* **1993**, *13*, 135–146.

(58) Evanics, F.; Maurmann, L.; Yang, W. W.; Bose, R. N. Nuclear magnetic resonance structures of the zinc finger domain of human DNA polymerase-alpha. *Biochim. Biophys. Acta—Proteins Proteomics* **2003**, *1651*, 163–171.

(59) Volckova, E.; Evanics, F.; Yang, W. W.; Bose, R. N. Unwinding of DNA polymerases by the antitumor drug, cis-diamminedichloro-platinum(II). *Chem. Commun.* **2003**, 1128–1129.

(60) Anzellotti, A. I.; Liu, Q.; Bloemink, M. J.; Scarsdale, J. N.; Farrell, N. Targeting retroviral Zn finger-DNA interactions: A small-molecule approach using the electrophilic nature of trans-platinum-nucleobase compounds. *Chem. Biol.* **2006**, *13*, 539–548.

(61) Sartori, D. A.; Miller, B.; Bierbach, U.; Farrell, N. Modulation of the chemical and biological properties of trans platinum complexes: monofunctional platinum complexes containing one nucleobase as potential antiviral chemotypes. *J. Biol. Inorg. Chem.* **2000**, *5*, 575–583.

(62) Franzman, M. A.; Barrios, A. M. Spectroscopic evidence for the formation of goldfingers. *Inorg. Chem.* **2008**, *47*, 3928–3930.

(63) de Paula, Q. A.; Mangrum, J. B.; Farrell, N. P. Zinc finger proteins as templates for metal ion exchange: Substitution effects on the C-finger of HIV nucleocapsid NCp7 using M(chelate) species (M = Pt, Pd, Au). *J. Inorg. Biochem.* **2009**, *103*, 1347–1354.

(64) Larabee, J. L.; Hocker, J. R.; Hanas, J. S. Mechanisms of Aurothiomalate-Cys2His2 Zinc Finger Interactions. *Chem. Res. Toxicol.* **2005**, *18*, 1943–1954.

(65) Casini, A.; Cinellu, M. A.; Minghetti, G.; Gabbiani, C.; Coronnello, M.; Mini, E.; Messori, L. Structural and solution chemistry, antiproliferative effects, and DNA and protein binding properties of a series of dinuclear gold(III) compounds with bipyridyl ligands. *J. Med. Chem.* **2006**, *49*, 5524–5531.

(66) Casini, A.; Karotki, A.; Gabbiani, C.; Rugi, F.; Vasak, M.; Messori, L.; Dyson, P. J. Reactivity of an antimetastatic organometallic ruthenium compound with metallothionein-2: relevance to the mechanism of action. *Metallomics* **2009**, *1*, 434–441.

(67) Casini, A.; Mastrobuoni, G.; Ang, W. H.; Gabbiani, C.; Pieraccini, G.; Moneti, G.; Dyson, P. J.; Messori, L. ESI-MS characterisation of protein adducts of anticancer ruthenium(II)-arene PTA (RAPTA) complexes. *ChemMedChem* **2007**, *2*, 631–635.

(68) Ang, W. H.; Parker, L. J.; De Luca, A.; Juillerat-Jeanneret, L.; Morton, C. J.; Lo Bello, M.; Parker, M. W.; Dyson, P. J. Rational Design of an Organometallic Glutathione Transferase Inhibitor. *Angew Chem., Int. Ed.* **2009**, *48*, 3854–3857.

(69) Groessl, M.; Tsybin, Y. O.; Hartinger, C. G.; Keppler, B. K.; Dyson, P. J. Ruthenium versus platinum: interactions of anticancer metallodrugs with duplex oligonucleotides characterised by electrospray ionisation mass spectrometry. *J. Biol. Inorg. Chem.* **2010**, *15*, 677–688.

(70) Will, J.; Kyas, A.; Sheldrick, W. S.; Wolters, D. Identification of (eta(6)-arene) ruthenium(II) protein binding sites in E-coli cells by combined multidimensional liquid chromatography and ESI tandem mass spectrometry: specific binding of [(eta(6)-p-cymene)RuCl2-(DMSO)] to stress-regulated proteins and to helicases. *J. Biol. Inorg. Chem.* **2007**, *12*, 883–894.

(71) Khalaila, I.; Bergamo, A.; Bussy, F.; Sava, G.; Dyson, P. J. The role of cisplatin and NAMI-A plasma-protein interactions in relation to combination therapy. *Int. J. Oncol.* **2006**, *29*, 261–268.

(72) Scolaro, C.; Bergamo, A.; Brescacin, L.; Delfino, R.; Cocchietto, M.; Laurenczy, G.; Geldbach, T. J.; Sava, G.; Dyson, P. J. In vitro and in vivo evaluation of ruthenium(II)-arene PTA complexes. *J. Med. Chem.* **2005**, *48*, 4161–4171.

(73) Mestroni, G.; Alessio, E.; Sava, G. *New salts of anionic complexes of Ru(III) as antimetastatic and antineoplastic agents.* 1996.

(74) Huang, G. C.; Liu, S. Y.; Lin, M. H.; Kuo, Y. Y.; Liu, Y. C. The synergistic cytotoxicity of cisplatin and taxol in killing oral squamous cell carcinoma. *Jpn. J. Clin. Oncol.* **2004**, *34*, 499–504.

(75) Parks, B. A.; Jiang, L.; Thomas, P. M.; Wenger, C. D.; Roth, M. J.; Boyne, M. T.; Burke, P. V.; Kwast, K. E.; Kelleher, N. L. Top-down proteomics on a chromatographic time scale using linear ion trap Fourier transform hybrid mass spectrometers. *Anal. Chem.* **2007**, *79*, 7984–7991.

(76) Schaub, T. M.; Hendrickson, C. L.; Horning, S.; Quinn, J. P.; Senko, M. W.; Marshall, A. G. High-performance mass spectrometry: Fourier transform ion cyclotron resonance at 14.5 T. *Anal. Chem.* **2008**, *80*, 3985–3990.